Laser guide star adaptive optics at Lick Observatory

Donald Gavel, Renate Kupke, Daren Dillon, Andrew Norton, Chris Ratliff, Jerry Cabak, Andrew Phillips, Connie Rockosi, Rosalie McGurk, Srikar Srinath, Michael Peck, William Deich, Kyle Lanclos, John Gates, Michael Saylor, Jim Ward, Terry Pfister

University of California Observatories, Santa Cruz, CA

ABSTRACT

We present an overview of the adaptive optics system at the Shane telescope (ShaneAO) along with research and development efforts on the technology and algorithms for that will advance AO into wider application for astronomy. Diffraction-limited imaging and spectroscopy from ground based large aperture telescopes will open up the opportunity for unprecedented science advancement. The AO challenges we are targeting are correction down to visible science wavelengths, which demands high-order wavefront correction, and dim object viewing over the whole sky, which demands bright artificial laser beacons. We discuss our ongoing development of MEMS based AO correction, woofer-tweeter architecture, wind-predictive wavefront control algorithms and a guide star laser tuned for optical pumping of the sodium layer. We present the latest on-sky results from the new AO system and present status and experimental plans for the optical pumping guide star laser.

Keywords: Adaptive Optics, Laser Guidestar, MEMS Deformable Mirror, Woofer-Tweeter

1. INTRODUCTION

The Lick Observatory has been a pioneer in the application of adaptive optics for astronomical observing, and has had a sodium laser guidestar system operating at the observatory's 3-meter telescope since 1996.[1] In early 2011 we started construction of a second generation adaptive optics instrument and a new sodium guide star laser.[2] The new AO system, ShaneAO and its science camera ShARCS (Shane Adaptive Red Camera and Spectrometer) are now in regular science use at the telescope. The laser is in preparation in the Laboratory for Adaptive Optics (LAO) with plans to field it at the telescope in 2016.

The objective of our efforts at LAO are to demonstrate all-sky high-Strehl AO science down to visible wavelengths. The system is a precursor to ones planned for Keck and TMT. It is characterized by a high-order of wavefront correction using a MEMS deformable mirror, the use of laser guide star to enable high sky coverage for science, and partial AO sharpening of tip/tilt stars to improve sky coverage and resolution performance on dim science targets. The laser is designed to take maximum benefit of sodium atomic optical pumping to enhance return, and has a variable pulsed format that can enable blanking of the Rayleigh scatter background. The adjustable features of the laser will allow us to experiment with pulse and spectral formats that could improve the return efficiency (brightness per watt of laser power) over a traditional CW optical pumping laser. A theoretical sodium atomic return model has predicted a considerable improvement over the present dye laser system at Lick of at least a factor of 5x brighter guidestar for the same laser power. This brightness guide star should provide the AO wavefront sensor with enough light to provide AO correction down to $\lambda 0.7 \mu m$ before wavefront sensing noise becomes a dominant error budget contributor.

2. GUIDE STAR LASER

Design parameters for a guide star laser should be selected to optimize the AO instrument performance and science objectives against cost. Having the beacon at high altitude provides the best sampling of the atmosphere with a single beacon. Making the beacon small in angular extent makes the AO wavefront reconstruction easier since it then mimics a bright natural star star and provides best wavefront reconstruction signal to noise for a given total brightness. Finally, making the laser maximally efficient in its conversion to return signal is beneficial in terms of AO performance per dollar spent. There are also benefits to a pulsed laser which are explained below.

Send correspondence to D.G.: gavel@ucolick.org

These consideration favor a Sodium beacon for large telescope apertures. The Sodium layer is the highest terrestrial phenomenon that can be utilized to produce an artificial beacon, with the guidestar in the mesosphere at 90km altitude. For a 3-meter telescope like the Shane, a lower altitude Rayleigh guidestars (30km) would introduce significant cone effect error, whereas the cone effect from a 90km Sodium beacon is almost negligible. Larger aperture telescopes will of course start to see cone effect even with 90km sodium beacons. Hence the Keck and TMT (10 and 30 meter respectively) will need multiple beacons to overcome the dominant error contributor being cone effect. For the Shane telescope one guide star suffices. The Sodium resonance at 589 nm has the highest cross-section of any of the trace metals in the mesosphere and the light in the mid-visible where fast CCD detectors are sensitive.

Originally Sodium guide star lasers used at astronomical observatories were designed to produce light over the entire Doppler-broadened Sodium D2 line. The Sodium resonance is spread due to the range of atom radial velocities (red and blue shifted) at the 180°K temperature at the mesosphere. However, the broadened laser line approach does not couple laser light efficiently into individual atoms. Theoretical research and experimentation[3,4] showed that a single narrow CW line, if circularly polarized, optically pumps the atoms into a two-state transition oscillation and results in a much more efficient coupling of return to incident illumination, even though a narrow line addresses only a fraction of the Doppler broadened population. A wider line causes a down-pumping effect where the population falls into a D2b ground state, significantly reducing the resonant return. A number of other natural phenomena can compete with optical pumping, in particular collisions of the Sodium with other atoms (scrambling the atomic state) and Larmor precession where the earth's magnetic field scrambles the state. The latest design guide star lasers are CW having two narrow lines, one with 85% of the energy at D2a and the second with 15% at D2b. The D2b line performs a "cleanup" of those atoms that inadvertently fall into the D2b ground state, returning them to the optical pumping cycle. The lines are narrow, 10 MHz, so they address only the zero-radial velocity atoms, within the bandwidth of their resonance. Narrow line CW Sodium lasers with sufficient power are now commercially available, so they are being widely adopted by the AO community in near-term system planning.

Pulsed lasers offer system advantages however. The first obvious one is being able to time gate the return to block the Rayleigh backscatter coming from low altitudes, which is a significant source of noise in the wavefront sensing. Figure 1 show how this is done with a nominally 30 μs pulse on a 20% duty cycle. The pulse rate and duration will need to vary with zenith angle as the distance to the sodium layer changes with $sec\theta_z$. A 30 μs pulse is long enough to move atoms into the optical pumped condition, and may in fact be near an optimum time scale in terms of producing optical pumping ahead of the competing collisional and Larmor time scales. Simulations by Rampy[5] show a peak response in the 10's of μs pulse range (Figure 2).

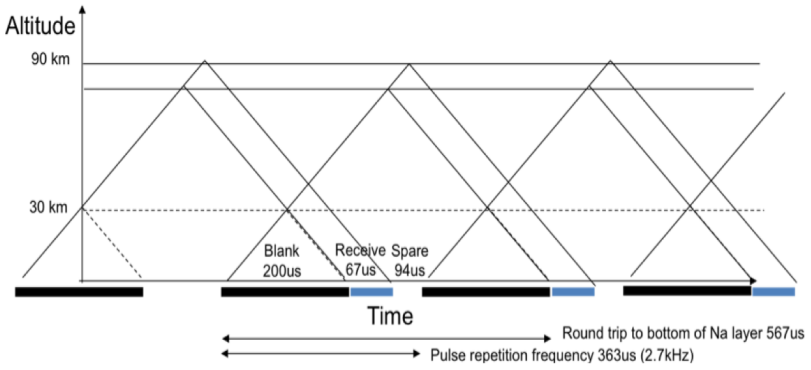

Figure 1. Timing diagram for a pulsed laser with gated return signal. The gate is open for return pulse from the Sodium layer, but closed during low-altitude Raleigh backscatter. There are continually two pulses in the air in this example, so a pulse is received twice per round-trip cycle, or at $1.67\cos\theta_z$ kHz.

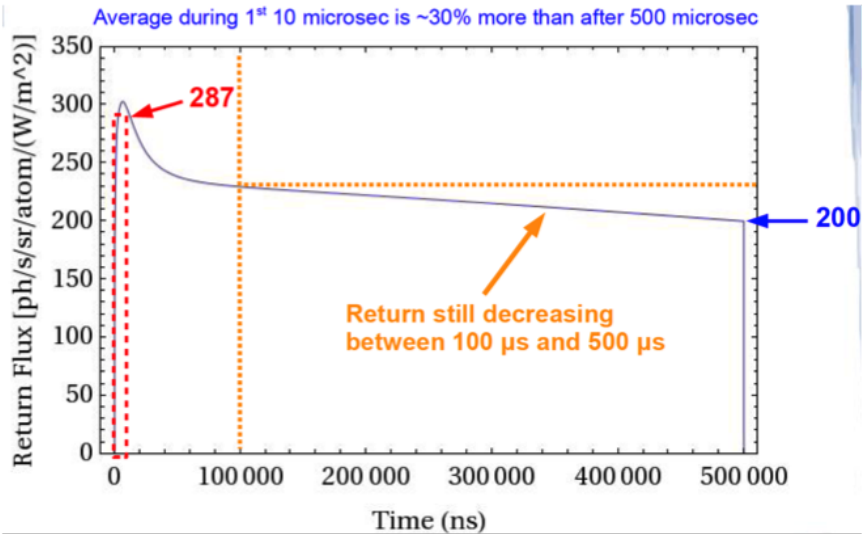

Figure 2. Theoretical prediction of guide star return flux vs pulse width (simulated results using the LGSBloch package). The curve implies that there is an optimal pulse duration where optical pumping wins out over competing processes to give the greatest flux return per laser watt.

The LAO is collaborating with Lawrence Livermore National Laboratory (LLNL) to field a fiber-optic technology laser at Lick. The laser was originally developed under an NSF Center for Adaptive Optics (CfAO) research grant and is now undergoing modification for incorporation with the ShaneAO system under the support of the Gordon and Betty Moore Foundation and UCO. The laser produces two high-power infrared lines, one at 1583 nm with an Erbium doped fiber amplifier and another at 938 nm with a Neodymium doped fiber amplifier, and combines the two lines in a nonlinear PPSLT (Periodically poled stoichiometric Lithium Tantalite) crystal to covert the infrared energy to 589 nm light. High conversion efficiency and output power were demonstrated at LLNL.[6] The laser has a programmable spectral and pulse format based on electro-optic modulators at the inputs of the amplifier chain. The seed light from commercial low-power lasers at 1583 and 938 nm is amplified in fiber amplifiers. In each case, the seed light propagates and gets amplified in the core of the fiber. Power is provided via light counter propagating in the cladding of the fiber, which along the path feeds energy to invert the population of dopant in the core.

The process of deployment at the observatory requires several engineering activities to make it suitable for operations in the observatory environment and in coordination with the ShaneAO system. These include a) rebuilding several laser couplings for stability and robustness, b) replacing the suite of older technology pump diodes which have degraded since the original experimentation, c) adding diagnostic systems for power and modulation monitoring, and pointing into the sum-frequency crystal, d) adding a modulator to produce the 15% energy D2b line (Figure 3), e) building a light-tight environmentally controlled enclosure for use at the observatory dome, f) adding laser safety interlock systems at the laser and in the observatory dome.

The laser will be housed in an enclosure on the dome mezzanine level, close to the telescope mounting fork. The 589 nm light will be transported via fiber to the laser launch telescope which is mounted on the side of the telescope. We plan to use a photonics crystal fiber built by Mitsubishi Cable, which is on long-term loan to us from Keck Observatory.

A particularly challenging new technology for the laser is the polarization-maintaining high power amplifier fiber for the 938 nm line. The fiber prescription was done at LLNL and the fiber manufactured by NuFern. We ran in to recent difficulties with the fiber originally pulled in 2007. The protective sheath was unfortunately pervious to water and O_2 leached into the cladding, causing significant absorption of the 808 nm pump light resulting in overheating and failure of the fiber. NuFern has since developed a new sheathing material and delivered a new fiber to us, for which we expect a longer lifetime. However, this set us back several months in

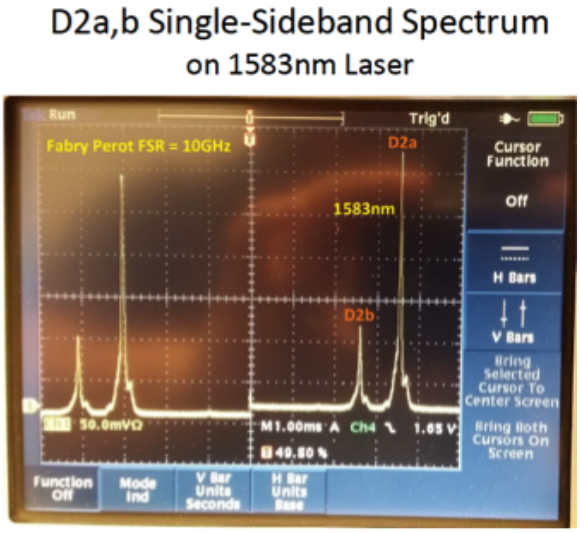

Figure 3. Results of modulating the laser to add a D2b repump line. The technique suggested by Hillman[7] was used to produce a single sideband at 1.7 GHz difference without producing a second energy-robbing sideband. (The picture shows two cycles of free-spectral range on the Fabry-Perot scanning interferometer used to measure the spectrum)

schedule and the laser is still in the laboratory undergoing testing. Our schedule now has us deploying at the observatory some time in the summer of 2016.

The nominal pulse format has a 20% duty cycle in order to boost conversion efficiency in the PPSLT crystal. This requires high instantaneous power in the fibers so to avoid SBS degradation, the seed is modulated to produce up to 9 lines. These are separated by roughly 100 MHz, far enough to avoid downpumping a neighboring Doppler classes in the Sodium layer, but close enough to get all the lines into the broadened spectrum. Each of these "picket-fence" lines has a corresponding D2b repump line (the D2b modulator is put ahead of the picked-fence modulator). In on-sky experiments we will be able to adjust this spacing; closer spacing gets to higher bin density (more resonant atoms) but at some point start to interfere with down-pumping.

A related issue is the beam transport via fiber. Split into several lines we should be able to avoid the SBS and other problems of high-power transport in the glass core so long as the fiber length is short. Scaling from the successful use of this fiber at Subaru Telescope with a 4 watt laser, and at VLT with a 10 watts split on 3 lines we are confident that we should be able to transport the estimated 22 meter path length. A huge advantage in this is that the coupling to the launch telescope will be deployable, so it can be shared with the existing dye laser and enable a side-by-side on-sky comparison.

Once the laser is deployed, we plan a series of experiments to measure the performance, validate the modeling, and investigate possible guidestar return-enhancing schemes. These tests include: a) vary the pulse width to investigate a possible optimum of optical pumping against competing processes, b) vary the line-spacing to investigate the trade between Sodium density and downpumping interference, c) do a side-by-side comparison of fiber laser, with its optically-pumping narrow lines / long pulses, against the existing dye laser with its short pulses and broadened spectrum. This may help resolve the discrepancy in the dye laser's expected return that has arisen in Rampy's simulations.[5] Additional experimentation is enabled by the laser's flexibility of pulse / spectral format, including: pulsing at the Larmor frequency (using a suggestion by Hillman[7]) and possibly adding a chirp to the modulation to follow atomic recoil.[8]

3. SHANEAO SYSTEM

The ShaneAO adaptive optics system with Shane Adaptive Red Camera and Spectrometer (ShARCS) science instrument is a diffraction-limited imager, spectrograph, coronagraph, and polarimeter for the visible and near infrared science bands. Adaptive optics corrects for the nominally ∼1 arcsecond seeing blur over an approximately

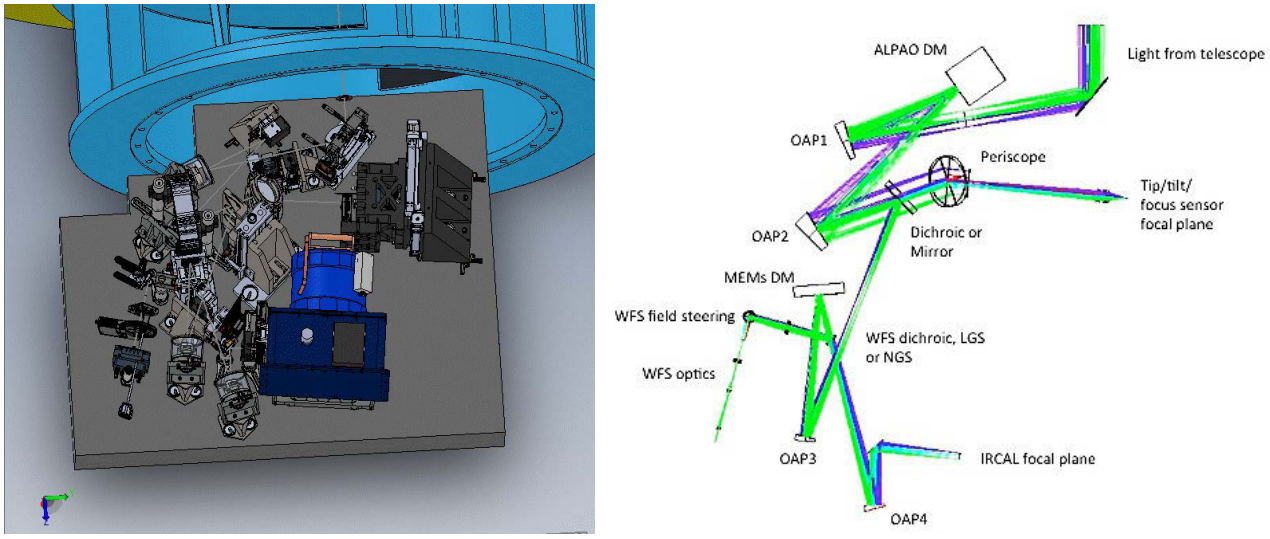

Figure 4. Computer renditions of the optomechanical layout(left) and optical paths (right) for ShaneAO.

20 arc second field of view, roughly matching the expected isoplanatic patch[9,10] in the longest science wavelength band. With the laser guidestar, the system has full sky coverage with performance dependent on proximity of a natural tip/tilt star, airmass, and seeing conditions.

The system features a woofer-tweeter architecture, with a Boston Micromacines 1020-actuator MEMS tweeter deformable mirror and an ALPAO DM52 membrane woofer deformable mirror. With this combination, the wavefront control rarely, if ever, saturates and the control response is entirely linear and predictable. A unique offloading woofer-tweeter control algorithm[11] provides the splitting of control between the two deformable mirrors.

The AO system optical layout is shown in 4. Further details of the opto-mechanical design can be found in[12]

Strehl performance with natural guidestars has been excellent. FIgure 5 compares the nominal predicted Strehl with ShaneAO compared to the prior AO system. Strehl performance on bright natural stars has been meeting these performance goals. Figures 6 and 7 show actual on-sky point-spread functions from ShaneAO in the near-infrared science bands. Figure 8 shows an AO corrected image of the planet Uranus. Similar images can be seen on the ShaneAO web page at http://lao.ucolick.org/ShaneAO/material/index.html.

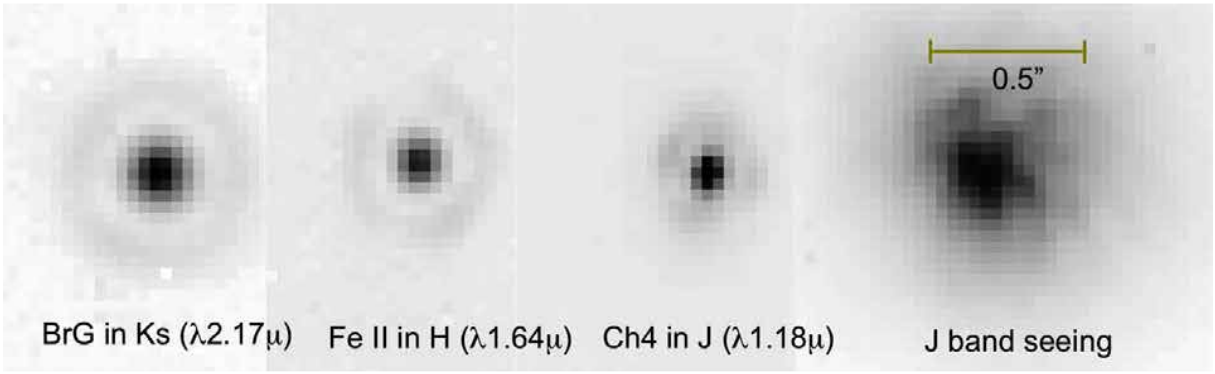

Figure 6. Point spread functions at each of the science bands.

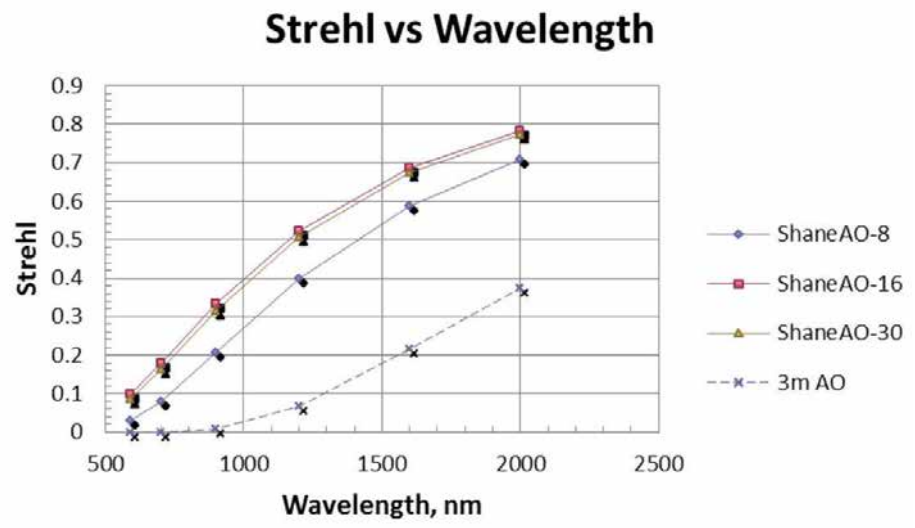

Figure 5. Predicted Strehl performance of ShaneAO and comparison to the older AO system at Lick.

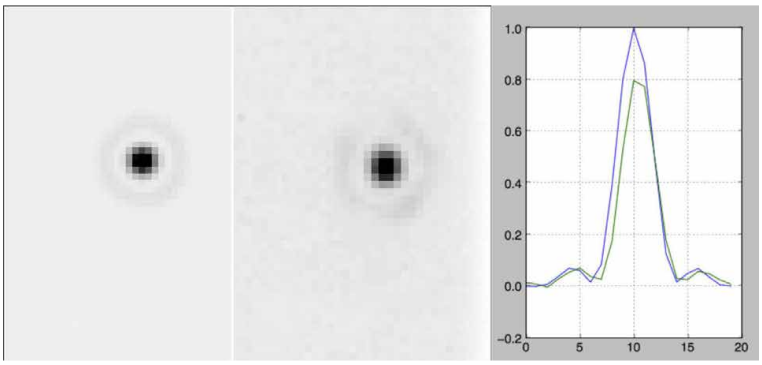

Figure 7. Left: PSF of internal source in H band (image-sharpened). Center: AO corrected H band PSF on sky. The on-sky Strehl is approximately 0.8 relative to the calibrator (lineout comparison on right).

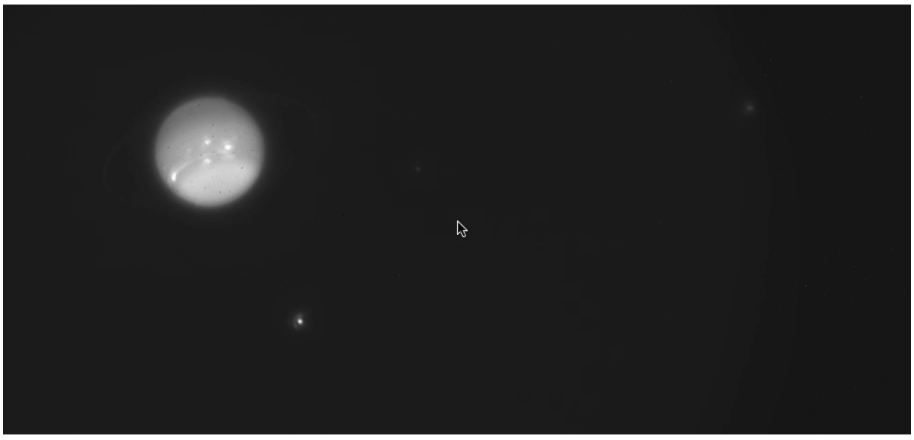

Figure 8. Image of Uranus, rings, and three orbiting moons. See the movie and other AO images at http://lao.ucolick.org/ShaneAO/material/index.html.

The AO system's wavefront and tip/tilt sensors provide excellent tools for characterizing Mount Hamilton seeing conditions that is independent of dome seeing and telescope optical aberrations. The Hartmann sensor can function as a differential image motion monitor (DIMM).[13] We filter out all the static and low-temporal frequency components to get an estimate of the atmospheric contribution to full-width-half-maximum (FWHM) and r_0. This can be corroborated with exposures of a star taken with the tip/tilt sensor. The tip/tilt sensor is located in the optical path after the woofer deformable mirror. This mirror can be set frozen to a long-term average of the wavefront correction in order to remove static and very slowly drifting aberration. With the AO loop open and this static correction applied, the resulting image is the PSF one would obtain through just atmosphere, with nearly perfect telescope and dome. Figure 9 shows FWHM with and without the static correction. The results imply that "native" seeing at Lick is actually quite good (we have data sets across several months showing similar behavior). In this case the statically corrected open seeing is 0.6 arcseconds as opposed to 0.9 arcseconds if there were no correction (DMs flat). The reported year-round seeing at Lick gleaned from the guider cameras has averaged about 1.25 arcseconds FWHM.

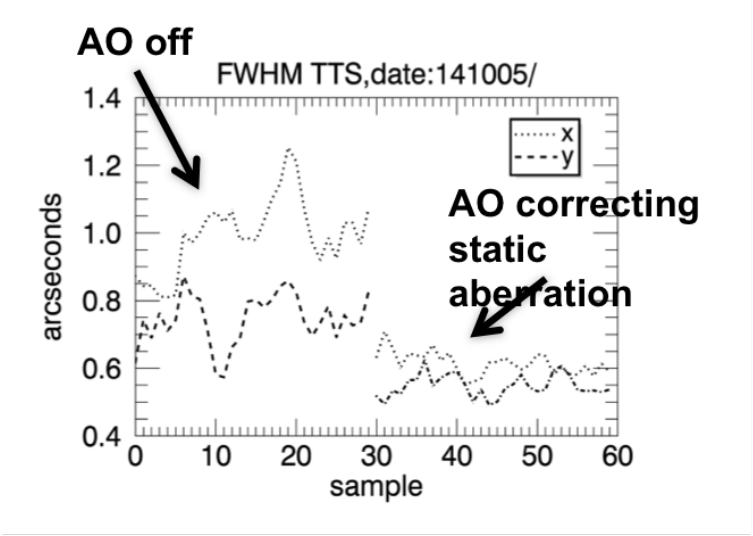

Figure 9. Measured seeing (full-width-half-max of a star) in the tip/tilt sensor, with AO off (left) and AO static correction only. The results imply a strong contribution of static and slowly drifting dome seeing components of wavefront error.

The isoplanatic angle, θ_0 characterizes the vertical profile of atmospheric turbulence. Because of turbulence at upper altitudes, the wavefront difference between guidestar and science target increases with angular separation. The K band θ_0 was very roughly determined using the old AO system to be about 20 arcseconds (corresponding to a 5 km mean height of turbulence[10]). This means that Strehl ratio should drop by a factor of $1/e$ at this separation. Figure 10 shows a ShaneAO K band image of the M92 star cluster, with the AO system locked on the 11'th magnitude star near the middle. In this image, the Strehl on-axis is about 0.8, and hardly drops off towards the edges of the field, implying that the isoplanatic angle, at least during this observation, is considerably larger, closer to $\theta_0 = 40$ arcseconds. A larger than expected isoplanatic angle would be consistent with a lower than expected upper atmospheric contribution to the aberrations. As discussed in the previous discussion, this can be explained by a large fraction of the nominal seeing being at the "ground" level in dome and telescope contribution.

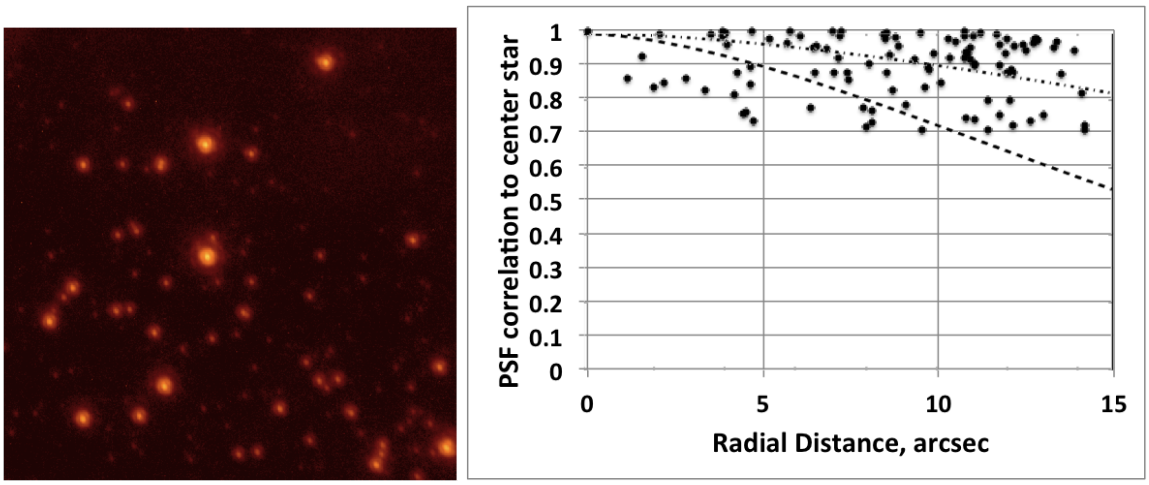

Figure 10. Left: the star cluster M92, with the AO system locked on the 11'th magnitude guide star near the middle. Right: the observed degradation in Strehl vs angular distance, normalized to one at zero separation angle. The dashed line is an expected fall-off due to anisoplanatism if θ_0 = 20 arcsec in K. The fall-off appears to be closer to one with a θ_0 = 40 arcsec (dotted curve).

The ShARCS spectroscopy mode in H and K bands was commissioned in early 2015 following repairs to mechanisms in the camera dewar. The slit position is now more mechanically repeatable and the grisms are better aligned with dispersion orthogonal to the slit. Figure 11 show initial measurements with a calibrator lamp and stars.

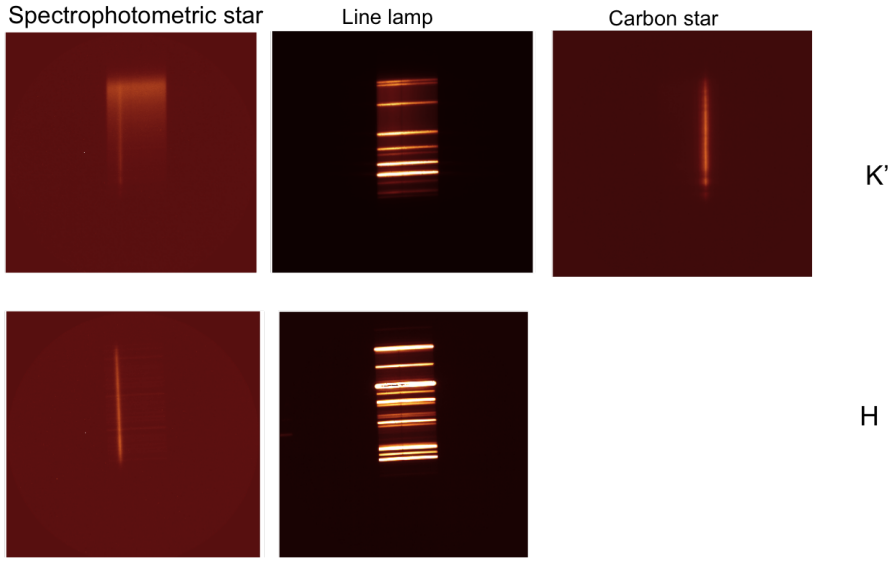

Figure 11. Raw spectra images with the K' and H band grisms, with (left to right) spectrophotometric calibration star, calibrator line lamp, and a star with spectra features.

4. CONCLUSION

An pulsed guide star laser is under development at the Lick Laboratory for Adaptive Optics that will take advantage of optical pumping of the Sodium atoms and have a variable pulse and spectral format that will allow other systematic improvements that will enhance signal-to-noise performance in the AO wavefront sensing. This

laser is presently in the laboratory with plans to field it at the observatory in the summer of 2016. We have completed the commissioning of the Shane adaptive optics system and infrared science camera on the telescope and continue with on-sky characterization and commissioning tests, including recently enabling the spectroscopic observing mode. The system is performing well, essentially as originally proposed, and represents a major step forward in AO capability for the observatory.

ACKNOWLEDGMENTS

This project was funded by the National Science Foundation, Major Research Instrumentation grant #0923585 (ShaneAO) and the Gordon and Betty Moore Foundation (Laser). The authors also gratefully acknowledge the support of the University of California Observatories who provided cost-sharing and in-kind contributions to the project.

REFERENCES

[1] C. E. Max, S. S. Olivier, H. W. Friedman, J. An, K. Avicola, B. V. Beeman, H. D. Bissinger, J. M. Brase, G. V. Erbert, D. T. Gavel, *et al.*, "Image improvement from a sodium-layer laser guide star adaptive optics system," *Science* **277**(5332), pp. 1649–1652, 1997.

[2] D. Gavel, "Development of an enhanced adaptive optics system for the Lick Observatory Shane 3-meter Telescope," *Proc. SPIE Photonics West* **7931**, 2011.

[3] P. W. Milonni, R. Q. Fugate, and J. M. Telle, "Analysis of measured photon returns from sodium beacons," *JOSA A* **15**(1), pp. 217–233, 1998.

[4] C. Denman, G. Moore, J. Drummond, M. Eickhoff, P. Hillman, J. Telle, S. Novotny, and R. Fugate, "Two-frequency sodium guide star excitation at the starfire optical range," in *CFAO, workshop*, 2006.

[5] R. Rampy, D. Gavel, S. M. Rochester, and R. Holzlöhner, "Toward optimization of pulsed sodium laser guide stars," *JOSA B* **32**(12), pp. 2425–2434, 2015.

[6] J. W. Dawson, A. D. Drobshoff, R. J. Beach, M. J. Messerly, S. A. Payne, A. Brown, D. M. Pennington, D. J. Bamford, S. J. Sharpe, and D. J. Cook, "Multi-watt 589nm fiber laser source," *Proc. SPIE* **6102**, pp. 61021F–61021F–9, 2006.

[7] T. J. Kane, P. D. Hillman, and C. A. Denman, "Pulsed laser architecture for enhancing backscatter from sodium," in *SPIE Astronomical Telescopes+ Instrumentation*, pp. 91483G–91483G, International Society for Optics and Photonics, 2014.

[8] E. Kibblewhite, "The Physics of the Sodium Laser Guide Stat: Predicting and Enhancing the Photon Returns," in *Advanced Maui Optical and Space Surveilance Technologies Conference*, 2009.

[9] D. L. Fried, "Varieties of isoplanatism," *Proc. SPIE* **0075**, pp. 20–29, 1976.

[10] E. Steinbring, S. Faber, B. Macintosh, D. Gavel, and E. Gates, "Characterizing the adaptive optics off-axis point-spread function. ii. methods for use in laser guide star observations1," *Publications of the Astronomical Society of the Pacific* **117**(834), pp. 847–859, 2005.

[11] D. Gavel and A. Norton, "Woofer-tweeter deformable mirror control for closed-loop adaptive optics: theory and practice," in *SPIE Astronomical Telescopes+ Instrumentation*, pp. 91484J–91484J, International Society for Optics and Photonics, 2014.

[12] D. Gavel, R. Kupke, D. Dillon, A. Norton, C. Ratliff, J. Cabak, A. Phillips, C. Rockosi, R. McGurk, S. Srinath, *et al.*, "Shaneao: wide science spectrum adaptive optics system for the lick observatory," in *SPIE Astronomical Telescopes+ Instrumentation*, pp. 914805–914805, International Society for Optics and Photonics, 2014.

[13] M. Sarazin and F. Roddier, "The eso differential image motion monitor," *Astronomy and Astrophysics* **227**, pp. 294–300, 1990.